due to an increase in the free energy of reaction by forming a relatively unstable cobalt(III) complex and/or a relatively stable MX^{n+} product. Other functions of bridging ligands (*e.g.*, changing the path of reaction, altering selection rules, varying the lifetimes of bridged intermediates, etc.) are much less obvious and will be considered elsewhere.

Acknowledgments. Support of this research by the National Science Foundation is gratefully acknowledged. We wish to thank Professors R. G. Linck and A. Haim for communicating some of their work prior to publication. It is a pleasure to express our appreciation for Professor Linck's many helpful comments and stimulating discussions.

Proton Magnetic Resonance Studies of Amino Acid Complexes of Platinum(II). I. Synthesis, Spectral Interpretation, and Conformational Implications[1]

Luther E. Erickson,[2] John W. McDonald,[3] John K. Howie,[4] and Roger P. Clow

Contribution from the Department of Chemistry, Grinnell College, Grinnell, Iowa.
Received March 23, 1968

Abstract: Proton nmr spectra of Pt(II) complexes of six different types of amino acids (**1–6**) have been analyzed. The effects of coordination and of proton titration on chemical shifts of skeletal protons and the presence or absence of ^{195}Pt side bands have been used to determine the coordination sites in multidentate ligands. Several different types of isomerism, including that resulting from creation of a new asymmetric center by coordination to the metal atom, are revealed by the spectra. A strong conformation dependence for ^{195}Pt–^{1}H spin coupling constants, which vary from about 10 to 60 Hz in Pt–N–C–H fragments, is suggested by the data. Simultaneous determination of J_{Pt-H} and J_{H-H} in several of the complexes indicates that J_{Pt-H} for Pt–N–C–H fragments is a maximum for dihedral angles (ϕ) near 180° and approaches a minimum for $\phi = 0°$. This conclusion is used to determine preferred conformations of other coordinated ligands.

As part of a study of stable diamagnetic complexes of nitrogen- and sulfur-containing ligands, we have synthesized several amino acid complexes of Pt(II) and have analyzed their proton nmr spectra. This paper (I) describes syntheses and analyses of proton nmr spectra of several of these complexes and discusses the ligand conformations which these data reveal. Separate papers describe subsequent studies of the kinetics of proton exchange and racemization of several complexes (II)[5] and the kinetics of inversion through sulfur in several complexes of S-methyl-L-cysteine (III).[6]

Structural formulas of the anion forms of the amino acids whose Pt(II) complexes (**1-6**) are described in this paper are given in Chart I. These particular compounds were chosen to represent a series of increasing complexity ranging from simple amino acids capable of N coordination or N, O chelation to compounds capable of forming a variety of complex species involving combinations of oxygen, nitrogen, and sulfur coordination.[7]

Chart I

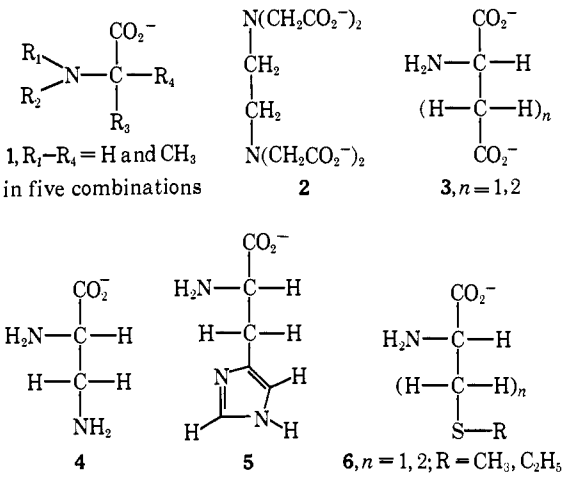

Several proton nmr studies of protonation sites and/or rotational conformations of these and similar amino acids have been reported.[8] Previously studied metal complexes of these amino acids range from labile[9]

(1) Portions of this work were reported at the 150th National Meeting of the American Chemical Society, Atlantic City, N. J., Sept 1965, and the 153rd National Meeting of the American Chemical Society, Miami Beach, Fla., April 1967.

(2) To whom correspondence should be addressed.

(3) National Science Foundation Undergraduate Research Participant, Summer 1966.

(4) National Science Foundation Undergraduate Research Participant, Summer 1965.

(5) L. E. Erickson, A. Dappen, H. Fritz, R. May, J. Uhlenhopp, and D. Wright, in preparation.

(6) L. E. Erickson and J. McDonald, in preparation.

(7) The following abbreviations will be used through this paper: glycinate = Gly^-, glycine·HCl = H_2Gly^+, glycine = HGly, etc.; alanine = HAla; sarcosine = HSar; α-aminoisobutyric acid = HAbu; N,N-dimethylglycine = HDmg; α,β-diaminopropionate = Dap^-; aspartate = Asp^{2-}; glutamate = Glu^{2-}; histidine = HHist; S-methylcysteine = HS-MeCys; methionine = HMet; S-ethylcysteine = HS-EtCys.

(8) (a) A. Nakamura and N. K. Zasshi, *J. Chem. Soc. Japan*, **86**, 780 (1965); (b) R. B. Martin and R. Mathur, *J. Am. Chem. Soc.*, **87**, 1065 (1965); (c) J. A. Glasel, *ibid.*, **87**, 5472 (1965); (d) K. G. R. Pachler, *Z. Anal. Chem.*, **224**, 211 (1966); (e) C. C. J. Calvenor and N. S. Ham, *Chem. Commun.*, 537 (1966); (f) J. R. Cavanaugh, *J. Am. Chem. Soc.*, **89**, 1558 (1967).

(9) (a) N. C. Li, R. L. Scruggs, and E. D. Becker, *ibid.*, **84**, 4650 (1962); (b) P. Taddei and L. Pratt, *J. Chem. Soc.*, 1553 (1964).

to stable[10] paramagnetic complexes and from labile[8b,9a,11,12] to stable diamagnetic complexes, including several studies of Co(III)[13-15] and EDTA[16-18] complexes. In diamagnetic complexes,[11-18] shifts due to metal complexing are of the same order of magnitude as shifts due to protonation. Furthermore, skeletal protons near coordination or protonation sites are usually most influenced by coordination or protonation. For platinum complexes, the presence or absence of side bands due to spin coupling to ^{195}Pt ($I = {}^1/_2$, 33% abundance) provides an additional spectral feature that can be employed to great advantage to establish coordination sites.[19]

After noting a substantial variation in J_{Pt-H} for Pt–N–C–H fragments of some of the first compounds investigated, we considered the possibility that these variations could be accounted for in terms of the conformation of the coordinated ligand. The dihedral angle of dependence of the vicinal coupling constant J_{H-H} in H–C–C–H fragments as calculated by Karplus[20] has been employed extensively in conformational analysis of substituted ethanes. Recent evidence indicates that the dihedral angle dependence of J_{H-F} for H–C–C–F fragments[21] and of J_{P-H} for P–C–C–H fragments[22] parallels that of J_{H-H}. While this paper was in preparation, Haake and Turley[23] reported work which indicated that the dihedral angle dependence of J_{Pt-H} for Pt–S–C–H fragments also parallels the Karplus calculations. In analyzing the conformational implications of our data, we have had the advantage of knowing J_{vic} for both H–C–C–H and Pt–N–C–H fragments of the same coordinated ligand, in several cases.

Experimental Section

Preparation of 1:1 Complexes from K_2PtCl_4. The following procedure evolved for the preparation of 1:1 dichloro complexes (*e.g.*, $KPtGlyCl_2$) of several amino acids. Equimolar mixtures of K_2PtCl_4 and the neutral amino acid were heated on a steam bath after being dissolved separately in water (about 10 ml/mmol of compound). After heating for 0.5 hr, the pH dropped to about 2.5. Potassium hydroxide solution (0.1 *N*) was then added to bring the pH to 4. The heating–titration cycle was repeated until 1 mequiv/mmol of amino acid had been added.

After rotary evaporation to dryness, the yellow 1:1 product was extracted from other solid reaction products with hot 90% ethanol (about 15 ml/mmol of Pt in three portions). Upon cooling in an ice bath, yellow crystals of 1:1 complex precipitated. One recrystallization from 90% ethanol–water was sufficient to eliminate KCl.

Preparation and Separation of *cis*- and *trans*-Pt(L-Dap)$_2$. The *cis* and *trans* isomers resulting from bidentate chelation through both nitrogens were obtained in comparable yields from the same reaction mixtures. In a typical preparation, 2.00 mmol (0.831 g) of K_2PtCl_4 and 4.00 mmol (0.563 g) of Dap·2HCl were dissolved in 20 ml of water and heated for several hours on a steam bath. At regular intervals during the heating, 0.1 *N* KOH was added to titrate amine protons displaced by platinum. Care was taken to keep the pH below 4 until the reaction was 90% completed. As the reaction proceeded, the color gradually changed from red to yellow to colorless. The addition of the last milliequivalent of base increased the pH to 9. On subsequent heating, the pH stabilized at 6 and some white solid appeared. The reaction mixture was then rotary evaporated to 6–7 ml, cooled in an ice bath, and centrifuged to remove the virtually insoluble white solid which was present. The separated solid was washed with five 0.5-ml portions of cold water and dried over P_2O_5 *in vacuo*, yield 53%. *Anal.* Calcd for $Pt(C_3H_7N_2O_2)_2$: C, 17.96; H, 3.52. Found: C, 17.55; H, 3.85.

The more soluble isomer was ultimately isolated as the dihydrochloride. It crystallized from a solution of the remaining dried reaction mixture in 2 ml of 12 *M* HCl. These crystals were separated by centrifugation, washed with two 0.5-ml portions of cold 12 *M* HCl and four 0.5-ml portions of ethanol, and dried *in vacuo* at 60°, yield 40% (93% for combined products). *Anal.* Calcd for $Pt(C_3H_7N_2O_2)_2 \cdot 2HCl$: C, 15.2; H, 3.41; N, 11.81; neut equiv, 237. Found: C, 15.64; H, 3.44; N, 11.55; neut equiv, 236 ±1.

The latter (more soluble) isomer is probably the *trans* isomer. It would be expected to have greater solubility because it has both CO_2^- groups on the same side of the coordination plane. The *cis* isomer, with CO_2^- groups on opposite sides of the coordination plane, could crystallize in a more stable configuration in spite of lower symmetry with respect to the coordinated nitrogens.

Preparation and Separation of Isomers of Pt(L-Hist)$_2$. The following procedure was followed to separate the two isomers, referred to here as *less soluble* and *more soluble* Pt(L-Hist)$_2$, and to obtain analytical and nmr samples: 12 mmol of histidine was added to 4 mmol of K_2PtCl_4 in about 80 ml of water. The reaction mixture was warmed to 60° and 0.1000 *N* NaOH was added to maintain the pH at 7.5. Approximately 1 hr was required to complete the addition of 80 ml, after which the pale amber solution was heated for another 30 min with only a slight drop in pH and the solution was concentrated to 15 ml by rotary evaporation. The less soluble Pt(L-Hist)$_2$ isomer which formed a colorless gelatinous precipitate, on standing, was removed by centrifuging and the mother liquor was evaporated to dryness. The precipitate was washed with five 2-ml portions of water, three 2-ml portions of methanol, and two 2-ml portions of ether and dried *in vacuo* at 60° for several hours.

The more soluble isomer was subsequently isolated from the remainder of the reaction mixture as the sulfate salt of the protonated species by treatment of the solid with 5 ml of 2 *M* H_2SO_4. The solid dissolved readily but, upon standing, a white solid precipitated. This precipitate was separated by centrifuging, washed twice with 1.5-ml portions of 2 *M* H_2SO_4, three times with 1-ml portions of cold water, three times with 2-ml portions of ethanol, and twice with 2-ml portions of ether, and dried *in vacuo* at 60° for several hours.

Repeated attempts to obtain reproducible (within ±10%) analytical data (C, H, and N analysis or equivalent weights) to confirm the assigned formulas, Pt(L-Hist)$_2$ and $H_2Pt(L\text{-Hist})_2 \cdot SO_4$, were unsuccessful. The assignment of formulas given is ultimately based on titration data of reaction mixtures and the nmr spectra of the isolated species.

Nmr spectra were obtained by dissolving the neutral (less soluble) or cationic (more soluble) complex in D_2O and enough 2.75 *M* NaOD to titrate both carboxyl and imidazole nitrogens ($pK_a \approx 10.5$) to convert to the anionic form. The solutions were then taken to dryness and redissolved in enough D_2O to give a final concentration of ~0.3 *M*. Since the cationic form of the more soluble complex has limited water solubility, spectra of supersaturated solutions were obtained by adding two to three drops of 33 *N* D_2SO_4 to the anion form in the nmr tube and recording two to three sweeps before

(10) A classic example is reported by C. C. McDonald and W. D. Phillips, *J. Am. Chem. Soc.*, **85**, 3736 (1963).
(11) R. H. Carlson and T. L. Brown, *Inorg. Chem.*, **5**, 268 (1966).
(12) R. J. Kula, D. T. Sawyer, S. I. Chan, and C. M. Finley, *J. Am. Chem. Soc.*, **85**, 2930 (1963).
(13) J. I. Legg and D. W. Cooke, *Inorg. Chem.*, **4**, 1576 (1965), and earlier papers cited therein.
(14) D. A. Buckingham, L. G. Margilli, and A. M. Sargeson, *J. Am. Chem. Soc.*, **89**, 825 (1967), and several earlier papers.
(15) R. G. Denning and T. S. Piper, *Inorg. Chem.*, **5**, 1056 (1966).
(16) Y. O. Aochi and D. T. Sawyer, *ibid.*, **5**, 2085 (1966).
(17) R. J. Kula, *Anal. Chem.*, **38**, 1581 (1966).
(18) J. L. Sudmeier and C. N. Reilley, *Inorg. Chem.*, **5**, 1047 (1966), and R. J. Day and C. N. Reilley, *Anal. Chem.*, **37**, 1326 (1965), discuss in considerable detail metal–EDTA systems and the effects of exchange rates, including partial unwrapping of the ligand, on the nmr line shapes.
(19) As a *rough* rule of thumb, J_{H-Pt} in σ-bonded ligands decreases by about an order of magnitude per additional bond from 1000 Hz for hydride complexes. See, for example, J. W. Emley, J. Feeney, and L. H. Sutcliffe, "High Resolution NMR Spectroscopy," Pergamon Press, New York, N. Y., 1966, p 1097.
(20) M. Karplus, *J. Am. Chem. Soc.*, **85**, 2870 (1963); *J. Chem. Phys.*, **30**, 11 (1959).
(21) K. L. Williamson, Y. F. Li, F. H. Hall, and S. Swager, *J. Am. Chem. Soc.*, **88**, 5678 (1966).
(22) C. Benzra and G. Ourisson, *Bull. Soc. Chim. France*, 1820 (1966).
(23) P. Haake and P. Turley, *J. Am. Chem. Soc.*, **89**, 4611, 4617 (1967).

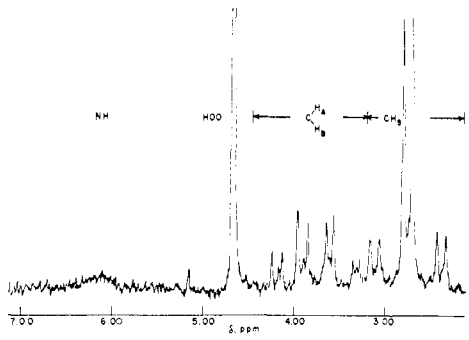

Figure 1. Proton nmr spectrum of a freshly prepared solution of the sarcosine complex $K(Pt(NHCH_3CH_2CO_2)Cl_2)$ in 0.01 M D_2SO_4.

significant precipitation of the sulfate salt occurred. Spectra of the more soluble species at low pH were obtained either by acidifying a high pH sample or by dissolving the neutral compound in 2 M D_2SO_4.

Preparation of S-Methyl and S-Ethyl Cysteine Complexes. The techniques employed to prepare $HPt(S\text{-}MeCyst)Cl_2$, $Pt(S\text{-}MeCyst)NH_3Cl$ (nitrogens *cis*), and $(Pt(S\text{-}MeCyst)(NH_3)_2)Cl$ and corresponding complexes of S-ethylcysteine were parallel to those used by Volshtein and Mogilevkina[24] in the preparation of corresponding complexes of methionine. $HPt(S\text{-}MeCyst)Cl_2$ was prepared by simply dissolving equimolar amounts of K_2PtCl_4 and S-methylcysteine in water and heating on a steam bath for a few minutes. After concentrating the solution to about 5 ml/mmol of product and cooling in an ice bath, $HPt(S\text{-}MeCyst)Cl_2$ precipitated as a yellow solid which was washed three times with cold water and dried *in vacuo* at 5°. Typical yields were 85–90%. *Anal.* Calcd for $Pt(C_4H_9NO_2S)Cl_2$: C, 11.98; H, 2.26; N, 3.49; neut equiv, 401. Found: C, 11.56; H, 2.62; N, 3.17; neut equiv, 410 ± 3.

Equivalent weights were obtained by rapid potentiometric titration of the complex dissolved in a concentrated KCl solution to retard hydrolysis of chlorides. $Pt(S\text{-}MeCyst)NH_3Cl$ and $(Pt(S\text{-}MeCyst)(NH_3)_2)Cl$, respectively, were prepared by treatment of aqueous solutions of $HPt(S\text{-}MeCyst)Cl_2$ with a stoichiometric amount and a large excess of aqueous ammonia. The latter, a very soluble white compound, was not isolated from the ammonium chloride produced in the reaction. $(Pt(S\text{-}MeCyst)en)Cl$ was prepared by adding 1 mmol each of ethylenediamine and NaOH to 1 mmol of $HPt(S\text{-}MeCyst)Cl_2$ in an aqueous solution.

Preparation of Previously Reported Complexes. Details of the preparation of the other compounds discussed in this paper are described in the literature. These include H_2PtGly_4,[25] *trans*-$H_2Pt(Asp)_2$, and *trans*-$H_2Pt(L\text{-}Glu)_2$,[26] and $H_2Pt(EDTA)Cl_2$ and $H_2PtEDTA$.[27]

Recording Spectra. Spectra were recorded with a Varian A-60 proton nmr spectrometer equipped with a temperature-control probe.

pH Measurements. All pH measurements were made with a Metrohm 300 pH meter, using a combination microelectrode which permitted measurement of the pH of the nmr samples themselves, when necessary. Potentiometric titrations were done with a Metrohm combitrator equipped with macroburet and Dosigraph.

Deuterated Solvents and Preparation of Samples. For most samples, D_2O solutions were prepared by dissolving the sample in 99.7% D_2O (Brinkman Instruments), rotary evaporating to dryness at 40–50° to reduce magnitude of HDO peak, and redissolving in D_2O. Several different stock solutions of NaOD, DCl, and D_2SO_4, prepared from concentrated stock solutions (Brinkman Instruments), were used to titrate nmr samples directly in nmr tubes or in the test tubes supplied with the combination microelectrode.

Chemical Shift Measurements. Chemical shifts were all measured with respect to either internal tetramethylammonium chloride

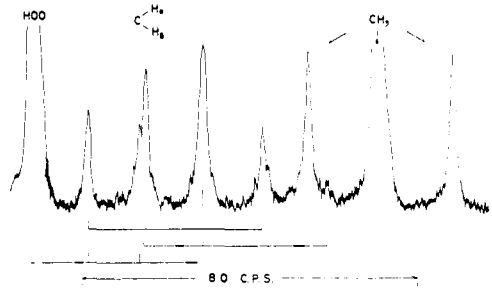

Figure 2. Proton nmr spectrum of the sarcosine complex $K(Pt(NDCH_3CH_2CO_2)Cl_2)$ in D_2O.

(TMA^+) or $(CH_3)_3Si(CH_2)_3SO_3Na$–NaTMS. The difference between the two standards (3.27 ppm) was used to convert all values to the NaTMS standard.

K_2PtGly_4–K_2PtCl_4 Equilibration Study. Stock solutions (0.25 M) of K_2PtCl_4 and K_2PtGly_4 in D_2O were prepared. Varying ratios of the two stock solutions were mixed in nmr tubes and thermostated at the desired temperature (50–70°). The temperature-controlled probe of the spectrometer was used to maintain a constant temperature while spectra were being recorded.

Results

The spectrum of $KPtGlyCl_2$ dissolved in 0.01 M DCl consists of a broad NH_2 signal at 5.38 ppm, the HDO signal, and a CH_2 triplet (6.6-Hz spacing between components) at 3.65 ppm. The CH_2 triplet decreases in intensity with time as a doublet (6.6 Hz spacing) due to $Pt(NHD\text{–}CH_2\text{–}CO_2)Cl_2^-$ becomes evident. At later times, or upon raising the pH, the NH_2 protons exchange completely and the CH_2 signal is a broad singlet. Symmetric ^{195}Pt side bands surround the CH_2 peak. Similar features are evident in the spectra of the other 1:1 complexes. However, the spectrum of the $PtSarcCl_2^-$ is more complicated and requires a more detailed description.

The spectrum of $PtSarcCl_2^-$, freshly dissolved in 0.01 M D_2SO_4, is shown in Figure 1. As noted by Halpern, Sargeson, and Turnbull, for a similar Co complex,[28] the two methylene protons are not equivalent. As a result, the CH_2 pattern consists of the eight lines typical of the AB part of an ABX spectrum, with X being the N–H proton at 5.97 ppm. In addition, weaker peaks due to the ^{195}Pt side bands of the CH_2 protons are evident, if indistinct. The methyl proton spectrum consists of a doublet, due to N–H proton coupling, flanked by symmetric doublet ^{195}Pt side bands. The CH_2 spectrum was analyzed to obtain ν_A, ν_B, J_{AX}, J_{BX}, and J_{AB}.

At higher pH, the N–H proton was rapidly replaced by deuterium and the eight-line AB portion of an ABX spectrum collapsed to a four-line AB pattern characterized by the same J_{AB}, ν_A, and ν_B (Figure 2). At this point, it was possible to assign frequencies to the eight additional peaks expected for the upfield and downfield ^{195}Pt side bands (AB part of ABX spectrum with X = Pt). The asymmetry in the appearance of the AB quartet and associated weaker side bands indicates that $J_{Pt-H_A} \neq J_{Pt-H_B}$. For our analysis we assumed that J_{Pt-H_A} and J_{Pt-H_B} have the same sign.[29] The assignment which best fits the observed spectrum is shown in Figure 2. The decision as to which CH_2 proton

(24) L. M. Volshtein and M. F. Mogilevkina, *Dokl. Akad. Nauk SSSR*, **142**, 1305 (1962); **163**, 1385 (1965).
(25) A. A. Grinberg and L. M. Volshtein, *Chem. Abstr.*, **29**, 6860 (1935).
(26) A. A. Grinberg and N. N. Katz, *Izv. Sektora Platiny i Drug. Blagorodn. Metal. Inst. Obshch i Neorgan. Khim. Akad. Nauk SSSR*, **29**, 37 (1955).
(27) D. H. Busch and J. C. Bailar, Jr., *J. Am. Chem. Soc.*, **78**, 716 (1956).
(28) B. Halpern, A. M. Sargeson, and K. R. Turnbull, *J. Am. Chem. Soc.*, **88**, 4630 (1966).
(29) In contrast to $(Pt(C_2H_5)_3Cl)_4$ for which J_{Pt-CH_2} and J_{Pt-CH_3} have opposite signs. See S. F. A. Kettle, *J. Chem. Soc.*, 6664 (1965).

Table I. Proton Chemical Shifts[a] of Glycine, Methyl-Substituted Glycines, and 1:1 Platinum (II) Complexes

Species	δ_{CH} or δ_{CH_2}	δ_{C-CH_3}	δ_{N-CH_3}	δ_{N-H}
H_2Gly^+	4.07 (0.84)			
$HGly^{+-}$	3.76 (0.53)			
Gly^-	3.23			
H_2Sar^{+-}	4.07 (0.88)		2.89 (0.52)	
$HSar^{+-}$	3.70 (0.51)		2.82 (0.45)	
Sar^-	3.19		2.37	
H_2Dmg^+	4.22 (1.15)		3.09 (0.77)	
$HDmg^{+-}$	3.81 (0.74)		3.01 (0.69)	
Dmg^-	3.07		2.32	
H_2Ala^+	4.30 (0.87)	1.65 (0.38)		
$HAla^{+-}$	3.83 (0.40)	1.53 (0.26)		
Ala^-	3.43	1.27		
H_2Abu^+		1.68 (0.38)		
$HAbu^{+-}$		1.56 (0.26)		
Abu^-		1.30		
$PtGlyCl_2^-$	3.65 (0.42)			5.38
$PtSarCl_2^-$	A = 3.48 (0.29)		2.71 (0.34)	5.97
	B = 3.98 (0.77)			
$PtDmgCl_2^-$	3.76 (0.69)		2.94 (0.62)	
$PtAlaCl_2^-$	3.82 (0.39)	1.48 (0.21)		?
$PtAbaCl_2^-$		1.56 (0.26)		5.52

[a] Chemical shifts throughout this paper are in parts per million downfield from internal $(CH_3)_3SiCH_2CH_2SO_3Na$–NaTMS. Values in parentheses are shifts relative to the corresponding amino acid anion. All measurements were made on D_2O solutions (0.25–0.50 *M*).

Table II. Proton–Proton and ^{195}Pt–Proton Spin Coupling Constants[a] of Chelated 1:1 Complexes of Glycine and Methyl-Substituted Glycines

Species	J_{H-C-H}	J_{H-C-CH_3}	$J_{H-C-N-H}$	$J_{Pt-N-C-H}$	$J_{Pt-N-CH_3}$	J_{H-N-CH_3}
$PtGlyCl_2^-$			6.6	38.5		
$PtSarCl_2^-$	17.00		4.5 (AX)	38.5 (H_A)	43.5	6.0
			6.5 (BX)	33.5 (H_B)		
$PtDmgCl_2^-$				33.7	36.2	
$PtAlaCl_2^-$		7.2	?	?		

[a] Coupling between ^{195}Pt and C–CH_3 is less than 0.5 Hz. Coupling between ^{195}Pt and N–H was not distinguished in the broad N–H proton resonance signals. All values are in hertz.

lies upfield cannot be made unequivocally. However, of the two methylene protons, the one which is more upfield (designated H_A) is the one which is more strongly coupled to ^{195}Pt (38.5 *vs.* 33.5) and more weakly coupled to H_X (4.5 *vs.* 6.5).

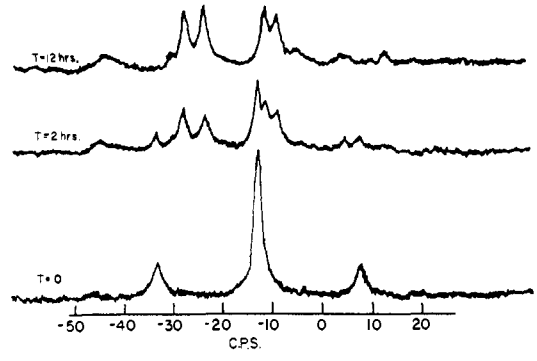

Figure 3. Nmr monitoring of equilibration in the system $PtCl_4^{2-}$–$PtGly_4^{2-}$ for equimolar (0.125 *M* each) initial concentrations of $PtCl_4^{2-}$ and $PtGly_4^{2-}$ in D_2O at 50°.

Proton chemical shifts and spin coupling constants of glycine and four methyl-substituted glycines and their 1:1 dichloro complexes of Pt(II) are given in Tables I and II. Proton shifts of the protonated, zwitterion, and anion forms of the acids were obtained by recording spectra at pH <1, 6 and >12, respectively. Shifts relative to anion forms are given in parentheses.

Other Glycine Complexes. Reaction of K_2PtCl_4 with a large excess of glycinate leads to the tetraglycine complex $PtGly_4^{2-}$, which has all four nitrogens coordinated to Pt. The compound can be precipitated readily as H_2PtGly_4 by acidification with 2 equiv of acid per mole of complex. Its spectrum in D_2O at pH 7 (Figure 3, $T = 0$) consists of a 1:4:1 triplet due to the four equivalent CH_2 groups and their ^{195}Pt side bands. Although only 1 equiv of acid can be added before precipitation begins, the effect of the protonation is to produce a downfield shift of about 0.3 ppm/mol of proton/mol of glycine which is comparable to shifts resulting from protonation of the carboxyl group of the uncomplexed amino acid.

With a 3:1 ratio of glycinate to K_2PtCl_4, the reaction mixture contains mainly a 3:1 complex in which one glycinate is chelated and the other two are N coordinated. The spectrum at pH 7 consists of three equal intensity peaks, each flanked symmetrically by ^{195}Pt side bands. The three peaks can be assigned to three different kinds of glycines on the basis of chemical shifts alone. The two upfield peaks have shifts very similar to that of $PtGly_4^{2-}$, and the downfield peak to $PtGlyCl_2^-$. The effect of protonation on the chemical shifts confirms the assignments given in Table III. Addition of DCl in increments produces a substantial downfield shift (about 0.33 ppm) for the two upfield peaks, but has little effect on the downfield peak. The designation of the N-coordinated glycine with the smaller $J_{Pt-N-C-H}$ as the one which is *trans* to the nitrogen of the chelated glycinate is based on the following reasoning.

Table III. Proton Chemical Shifts and ^{195}Pt-Proton Spin Coupling Constants for Some Glycine Complexes of Pt(II)

Species	Ligand coordination	CH_2 pH 7	CH_2 Lower pH	$J_{Pt-N-C-H}$
$PtGlyCl_2^-$	Chelated	3.65	3.65 (pH 2)	38.5
$PtGly_3^-$	Chelated	3.72	3.74 (pH 2)	32
	N coord-*trans*[a]	3.45	3.79 (pH 2)	33
	N coord-*cis*[a]	3.40	3.72 (pH 2)	43
$PtGly_4^{2-}$	N coord	3.47	3.55 (pH 4[b])	42
HGly	Free	3.76 (pH 6)	4.07 (pH 0)	

[a] *cis* and *trans* refer to position with respect to N of chelated Gly. [b] This corresponds to 1 mequiv of acid/mol of $PtGly_4^{2-}$ or protonation of one-fourth of free carboxyl groups. H_2PtGly_4 precipitates when more acid is added.

H_2PtGly_4 loses glycine on heating to yield almost exclusively *cis*-$PtGly_2$, presumably *via* $HPtGly_3$. The preferential loss of the *trans*-N-coordinated glycinate probably reflects a weaker Pt–N bond. It seems reasonable that the variation in $J_{Pt-N-C-H}$ similarly reflects this difference.[30]

Neither *cis*- nor *trans*-$PtGly_2$ is sufficiently soluble in D_2O (nor in other solvents tried) to obtain a proton spectrum.

Equilibration of $PtGly_4^{2-}$ and $PtCl_4^{2-}$. It is known that both *cis*- and *trans*-$PtGly_2$ can be converted to $H_2PtGly_2Cl_2$, a sparingly soluble yellow solid, by treatment with hot concentrated HCl.[25,26] Attempts to dissolve these yellow solids in NaOD to obtain nmr spectra were uniformly unsuccessful, since the titrated species reverted to $PtGly_2$ almost immediately upon addition of the base. A series of equilibration experiments, inspired by similar investigations by Van Wazer and coworkers,[31] provided further evidence for the instability of N-coordinated species and additional insight into the mechanism by which *cis*- and *trans*-$PtGly_2$ are formed.

Typical traces monitoring the equilibration of a 1:1 ratio of K_2PtGly_4 and K_2PtCl_4 in D_2O (0.25 *M* Pt) at 50° are shown in Figure 3. Initially ($T = 0$) only the 1:4:1 triplet of $PtGly_4^{2-}$ is present. After 2 hr, the concentration of $PtGly_4^{2-}$ decreased while $PtGly_3^-$ (three main peaks at −29, −11, and −8 cps on the scale shown) and $PtGlyCl_2^-$ (main peak at −23 cps) increased a corresponding amount. After 12 hr, no more $PtGly_4^{2-}$ remained and the concentrations of $PtGly_3^-$ and $PtGlyCl_2^-$ were approximately equal. No $PtGly_2$ had yet precipitated. Over the course of the next 40 hr, the intensity of the peaks assigned to $PtGly_3^-$ and $PtGlyCl_2^-$ decreased slowly to about 30% of their 12-hr intensity as insoluble $PtGly_2$ precipitated. Heating for another 20 hr produced no further precipitation and no further decrease in peak intensities nor other changes in the nmr spectrum. The gray solid was removed by centrifuging, washed, and dried, yield 70 ± 5% of Pt, based on $PtGly_2$. This corresponded to the observed decrease in area of the nmr peaks.

Similar experiments were run at four other compositions at 50° and the whole series was repeated at 70°. For $PtGly_4^{2-}$:$PtCl_4^{2-}$ ratios of 2.5:1.5 and 1.5:2.5, the spectra revealed a fairly rapid equilibration to $PtGly_3^-$ and $PtGlyCl_2^-$, followed by a much slower precipitation of $PtGly_2$ and resultant changes in relative intensities of peaks. For ratios of 3:1 and 1:3, $PtGly_3^-$ and $PtGlyCl_2^-$, respectively, predominated and very little $PtGly_2$ precipitated. Over the whole range studied spectra could be accounted for entirely in terms of the three species $PtGly_4^{2-}$, $PtGly_3^-$, and $PtGlyCl_2^-$. No significant concentration of free glycine was observed.

Aspartic and Glutamic Acid Complexes. The spectra of both 1:1 and 2:1 complexes of L-aspartic and L-glutamic acids were obtained. Typical spectra of 2:1 complexes are shown in Figure 4. The α-proton signal of each consists of a triplet symmetrically flanked by Pt side band triplets. For $Pt(L\text{-}Asp)_2^{2-}$, the inner peak of each side band triplet apparently overlaps the outer peak of the parent triplet. The downfield portion of the complex multiplet of $Pt(L\text{-}Glu)_2^{2-}$ was assigned to the terminal CH_2 group on the basis of the similarity of the shift to that of the CH_2 of the $Pt(L\text{-}Asp)_2^{2-}$. Shifts of the two methylene groups were estimated by a first moment analysis. Chemical shifts and spin coupling constants are tabulated in Table IV.

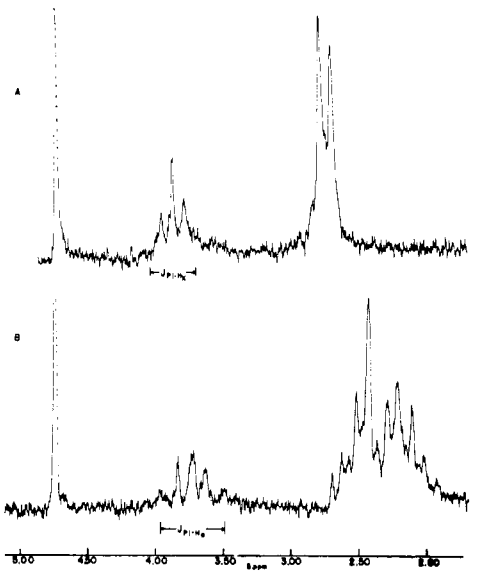

Figure 4. Proton nmr spectra of D_2O solutions: A, $Pt(L\text{-}Asp)_2^{2-}$; B, $Pt(L\text{-}Glu)_2^{2-}$.

trans 2:1 complexes of aspartic and glutamic acids prepared from L-amino acids might be expected to have simpler nmr spectra than corresponding complexes of DL-amino acids. For the latter, three possible 2:1 complexes need to be considered, DD, DL, and LL. Spectra of 2:1 complexes obtained from DL-aspartic or glutamic acids were essentially indistinguishable from those obtained from pure L isomers. It appeared,

(30) *Cf.* T. F. Bolles and R. S. Drago, *J. Am. Chem. Soc.*, **88**, 5730 (1966).

(31) For example, J. R. Van Wazer and S. Norval, *Inorg. Chem.*, **4**, 1294 (1965). See also L. M. Setz and T. L. Brown, *J. Am. Chem. Soc.*, **89**, 1607 (1967), and earlier papers cited therein.

Table IV. Proton Nmr Data for Aspartic and Glutamic Acids and Pt(II) Complexes

Species	pH	δ_X	$\delta_{BB'}$ [a]	δ_A, $\delta_{A'}$ [a]	J_{AX}, $J_{A'X}$	J_{Pt-HX}	$J_{AA'}$
H_3Glu^+	1	4.27	2.76	2.31	6.5		
$HGlu^-$	6	3.75	2.42	2.02	6.5		
Glu^{2-}	12	3.31	2.23	1.92	6.3		
$HPt(L\text{-}Glu)Cl_2^-$	2	3.78	2.73	2.26	6.3	31.2	
$Pt(L\text{-}Glu)Cl_2^-$	7	3.68	2.46	2.19	6.0	30	
$Pt(L\text{-}Glu)_2^{2-}$ [b]	9	3.73	2.46	2.19	5.7	26.7	
H_3Asp^+		4.56		3.26	5.3		?
$HAsp^-$	6	4.02		2.75, 2.89	9.6, 3.2		17.9
Asp^{2-}	12	3.63		2.36, 2.70	9.9, 3.8		15.5
$HPt(L\text{-}Asp)Cl_2^-$	2	4.06		3.00	5.1	?	?
$Pt(L\text{-}Asp)Cl_2^{2-}$	7	3.89		2.73	5.0	?	?
$Pt(L\text{-}Asp)_2^{2-}$ [b]	9	3.89		2.73, 2.78[c]	5.0	20.0	17.0

[a] Values for glutamic acid and its complexes were estimated by first moment method. A and A′ correspond to protons on the β position; B and B′, the α position. [b] Note: The spectra of the 2:1 complex as obtained from DL-glutamic or aspartic acids are indistinguishable from those of $Pt(L\text{-}Glu)_2^{2-}$ and $Pt(L\text{-}Asp)_2^{2-}$, respectively. [c] Separate values were obtained from a 100-MHz trace which showed all eight lines expected for the AB portion of an ABX pattern.

therefore, that differences in spectral parameters were not sufficient to permit this fairly subtle distinction. However, large solubility differences might have led to isolation of only one isomer. The following experiment provided additional evidence that the LL and DL 2:1 isomers in fact have essentially identical proton spectra at 60 MHz. It was observed that methine protons of all of the 1:1 and 2:1 complexes of aspartic and glutamic acids exchanged rapidly in D_2O at pH >12. The rates of racemization (determined polarimetrically) and of H_X proton exchange (determined by nmr) were measured simultaneously for several high pH samples of 2:1 LL complexes of both aspartic and glutamic acids. These rates were found to be identical.[5] Thereafter, the solutions were rotary evaporated to dryness, reprotonated by warming in H_2O at pH 12, acidified to pH 8, and reevaporated. Spectra of the racemic mixtures in D_2O, which now contained DL as well as DD and LL species, were essentially identical with those of the original LL 2:1 complexes.

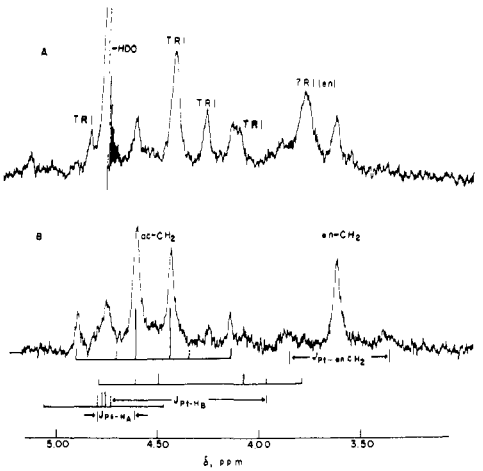

Figure 5. Proton nmr spectra of supersaturated solutions fo $H_4Pt(EDTA)Cl_2$ in (A) D_2O and (B) 6 *M* DCl recorded at magnet temperature (33°).

EDTA Complexes. Although potentially many different types of coordination are possible for EDTA, this investigation was confined to the well-characterized bidentate and tetradentate complexes designated here as $H_4Pt(EDTA)Cl_2$ and $H_2PtEDTA$, respectively.

The spectrum of a 0.3 *M* solution of $H_4Pt(EDTA)Cl_2$ in D_2O is shown in Figure 5A. It is far too complicated to be accounted for in terms of the two equivalent en-CH_2 and four equivalent ac-CH_2 groups present in the molecule, suggesting the presence of some tridentate or other species. Since ring closure would eliminate HCl, the equilibrium could be shifted toward $H_2Pt(EDTA)Cl_2$ by dissolving in DCl.

The spectrum of a supersaturated solution (~0.15 *M*) of $H_4Pt(EDTA)Cl_2$ in 6 *M* DCl is shown in Figure 5B. It consists of a low-field AB quartet (δ 4.38 and 4.63) and a broad high-field triplet (δ 3.64). The former can be assigned to the four identical acetate methylene groups and the latter to the four ethylenic protons and their ^{195}Pt side bands. The ^{195}Pt side bands of the acetate quartet are also evident, but are not symmetric with respect to the parent AB quartet because of unequal coupling of ^{195}Pt to H_A and H_B. As noted for $PtSarCl_2^-$, such unequal coupling is equivalent to an increase in the effective chemical shift difference for the upfield AB side band and to a decrease for the downfield AB side band. The assignment indicated schematically in Figure 5B corresponds to $J_{Pt-H_B} = 46$ and $J_{Pt-H_A} = 11$ Hz.

Having deciphered the spectrum of $H_4Pt(EDTA)Cl_2$, it was then possible to identify other peaks of the spectrum of the D_2O solution with the tridentate species, which has four nonequivalent acetate groups as well as four nonequivalent protons in the ethylenediamine (en) fragment. A tentative assignment of major tridentate peaks is shown in Figure 5A. The en-methylene protons are apparently not sufficiently different to give anything more complex than a broadened unresolved multiplet at 3.82 ppm.

The spectrum of tetradentate $H_2PtEDTA$ in D_2O at 90° is shown in Figure 6. It consists of three major absorption regions in addition to the solvent peak. Comparison with the bidentate spectrum and with extensive literature data[16-18] suggests that the most upfield peak is due to en-CH_2. The chelated and free acetate groups were assigned as shown in Figure 6 on the basis of the effect of titration on the chemical shifts. Although all peaks showed additional splittings when NaOD was added, only the peaks at 4.15 ppm moved upfield significantly. The amount of the upfield shift (~0.4 ppm) was comparable to the protonation shift of the bidentate aspartate or N-coordinated glycinate.

Table V. Proton Nmr Data for Three EDTA Complexes of Pt(II)

Species	ac-CH_2	en-CH_2	J_{AB}	J_{Pt-H_A}	J_{Pt-H_B}	$J_{Pt-enCH_2}$
$H_4Pt(EDTA)Cl_2$	4.72 (H_A) 4.38 (H_B)	3.64	17.8	11 ± 2	46 ± 2	29
$H_3Pt(EDTA)Cl$	4.43 (chel) 4.85 (free) 4.13 (free) 4.28 (free)	3.82				
$H_2Pt(EDTA)$	4.43 (chel)	3.95	17	(58 ± 5,	6 ∓ 5)	?

Table VI. Proton Nmr Data for L-α,β-Diaminopropionic Acid and Platinum(II) Complexes

Predominant species	pH	δ_X	δ_A	δ_B	J_{AB}	J_{AX}	J_{BX}	J_{Pt-H_X}	J_{Pt-H_A}	J_{Pt-H_B}
L-H_3Dap^{2+}	1.	4.46	(3.66)			(7.0)				
L-H_2Dap^{+}	3.7	4.34	(3.62)			(7.0)				
L-H Dap	7.1	3.86	(3.32)			(7.0)				
L-Dap^{-}	12	3.36	2.77	2.88	13.2	7.8	3.6			
cis-Pt(L-Dap)$_2$·2HCl	1	3.94	3.07	3.21	12.8	9.2	4.7	29.6	31.0	54.0
trans-Pt(L-Dap)$_2$·2HCl	1	4.00	3.06	3.23	12.8	9.8	4.8	26.4	28.4	56.4
trans-Pt(L-Dap)$_2$	7	3.71	2.88	3.09	12.6	10.5	4.0	28.0	30	55

Although ^{195}Pt side bands are not resolved for the whole spectrum, the chelated acetate peak has a distinct downfield pattern that can be recognized on the basis of relative intensities and spacings as three components of the downfield AB quartet side band. The

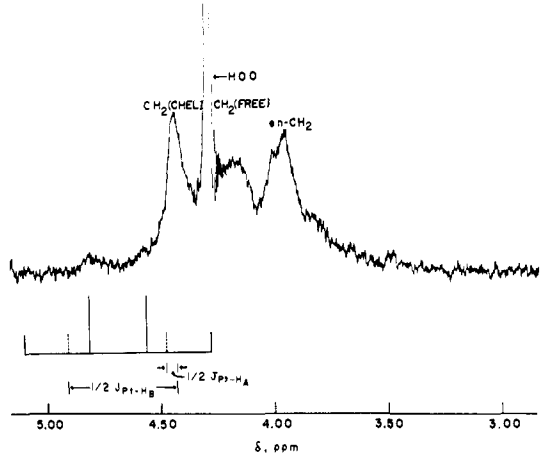

Figure 6. Proton nmr spectrum of saturated solution of $H_2Pt(EDTA)$ in D_2O recorded at 90° to shift HDO peak away from the ^{195}Pt side band.

situation here is just the reverse of that for $H_4Pt(EDTA)Cl_2$ for which the downfield side band is only an unresolved singlet while the parent acetate absorption is a well-defined AB quartet. The separation between the centers of the parent peak and the downfield quartet, 16 Hz, is just $^1/_4(J_{Pt-H_A} + J_{Pt-H_B})$. If $\delta_A = \delta_B$ for the parent spectrum, J_{Pt-H_A} and J_{Pt-H_B} = 58 and 6 Hz. Since the parent peak is fairly broad, $\nu_A - \nu_B$ could be up to about ±5 Hz. Since there is no way of knowing whether δ_A or δ_B is greater, J_{Pt-H_A} and J_{Pt-H_B} could be 58 ± 5 and 6 ± 5 Hz.

Chemical shifts and spin coupling constants for the three EDTA complexes are summarized in Table V.

L-α,β-Diaminopropionic Acid (Dap) Complexes. The spectrum of the less soluble 2:1 complex of L-α,β-diaminopropionic acid dissolved in DCl is shown in Figure 7. The α-proton quartet and four major components of the eight-line methylene (AB) portion of the expected ABX spectrum are clearly evident. However, location of the remaining four weaker peaks in the methylene part of the spectrum is complicated considerably by the presence of Pt side bands with unequal coupling between Pt and the three skeletal protons. The most obvious effect of unequal coupling is the more compressed appearance (essentially a doublet) of the upfield methylene side band in contrast to the more spread out appearance for the parent and downfield AB side band. With that observation as a clue, two of the four outer methylene lines were identified and the parent ABX pattern was analyzed to obtain J_{AX}, J_{BX}, J_{AB}, ν_A, ν_B, and ν_X. Four strong lines in the downfield methylene side band were then tentatively

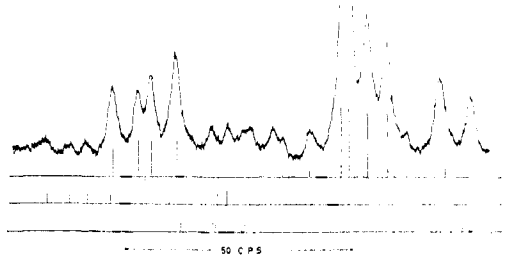

Figure 7. Analysis of 60-MHz proton nmr spectrum of $H_2(Pt(L\text{-}Dap)_2Cl_2)$ in D_2O.

identified. Again assuming that the sign of J_{Pt-H} is the same for all three ABX protons and that J_{AB} is the same for side bands as for parent ABX spectrum, the remaining four lines of the methylene portion of the downfield side band were located. Analysis of the downfield ABX side band spectrum, including methine quartet, yielded three chemical shifts. The differences between these shifts and the shifts for corresponding protons in the parent ABX spectrum is just $^1/_2J_{Pt-H}$ for these protons. Adding an equal amount to each parent proton shift yielded effective shifts for the three protons in the upfield side band. The upfield side band spectrum calculated from these effective shifts (along with J_{AX}, J_{BX}, J_{AB} obtained from analysis of the parent spectrum) is indicated schematically at the bottom of Figure 7.

Table VII. Proton Nmr Data for L-Histidine and Pt(II) Complexes in D_2O[a]

Predominant species	pH	δ_{C_2-H}	δ_{C_4-H}	δ_X	δ_{AB}	J_{AB}	J_{AX}, J_{BX}	J_{Pt-H_2}	J_{Pt-H_4}	J_{Pt-H_X}
H_3Hist^{2+}	1	8.83	7.62	4.68	3.65		(6.5)			
H_2Hist^{+}	4.0	8.72	7.33	4.12	3.37		(6.5)			
HHist	7.5	7.92	7.10	4.15	3.30		(6.5)			
$Hist^{-}$	13	7.80	7.03	3.65	3.00	14.2	9.0, 4.2			
cis-$H_2Pt(L\text{-}Hist)_2^{2+}$	1	8.10	7.32	3.95	3.33		(4.6)	16.1	8.8	46 ± 2
cis-$Pt(L\text{-}Hist)_2^{2-}$	12	7.53	6.97	3.38	3.12	15(?)	7.5, 3.4	8.6	8.0	33 ± 1
trans-$H_2Pt(L\text{-}Hist)_2^{2+}$	1	7.88	7.38	3.95	3.33		(4.6)	18.6	8.0	42 ± 2
trans-$Pt(L\text{-}Hist)_2^{2-}$	12	7.23	6.97	3.37	3.13	15(?)	8.0, 3.2	11.0	6.8	33 ± 1

[a] Values given are all for 0.2–0.4 *M* solutions at magnet temperature.

In order to provide a further check on the assignments given, the 100-MHz spectrum of $H_2Pt(L\text{-}Dap)_2Cl_2$ was computed by increasing all shifts by $^5/_3$, with the same six spin coupling constants. The calculated and observed 100-MHz spectra agreed within ±0.5 Hz at every major test point.

Chemical shifts and spin coupling constants of hydrochloride salts of both 2:1 isomers of Dap and of the high pH form of the more soluble (*trans*?) isomer are summarized in Table VI, which also includes parameters of diaminopropionic acid in its several charged forms. The latter were obtained by A_2X or ABX analysis of the spectra of the free acid. For the *trans* isomer in neutral form, it was impossible to locate sufficient lines to obtain J_{Pt-H_A} and J_{Pt-H_B} with high accuracy. However, the general appearance of the spectrum is very similar to that of the hydrochloride indicating large inequality between J_{Pt-H_A} and J_{Pt-H_B}.

cis **and** *trans* **Isomers of Pt(L-Hist)$_2$.** Spectra of the two isomers of $Pt(L\text{-}Hist)_2$ are shown in Figure 8.

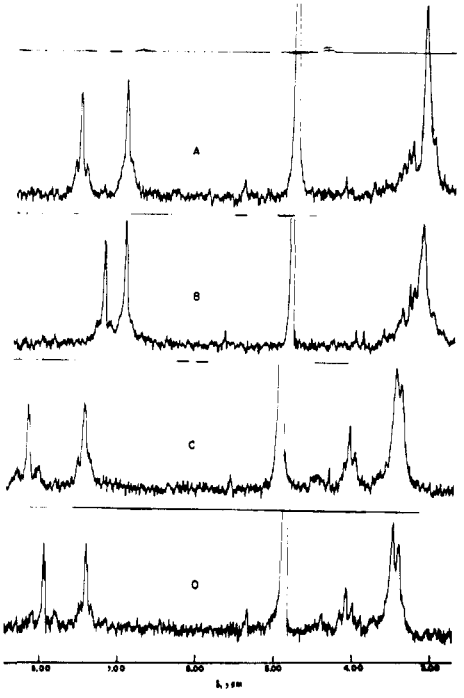

Figure 8. Proton nmr spectra of L-histidine complexes of Pt(II) in D_2O: A, *cis*-$Pt(L\text{-}Hist)_2$ at pH >12; B, *trans*-$Pt(L\text{-}Hist)_2$ at pH >12; C, *cis*-$Pt(L\text{-}Hist)_2$ at pH <0; D, *trans*-$Pt(L\text{-}Hist)_2$ at pH <0.

Each trace consists of downfield signals from the imidazole ring protons, the HDO signal, and upfield signals from the CH–CH_2 moiety. Each imidazole ring proton signal is a doublet ($J \approx 1$ Hz) symmetrically flanked by ^{195}Pt side bands at both high and low pH. However, the appearance of the CH–CH_2 portion of the spectrum changes significantly with pH. At low pH the CH–CH_2 spectrum of both isomers consists of a simple A_2X triplet-doublet, with relatively small coupling between protons and Pt side bands surrounding the H_X signal. By contrast, at high pH, the H_X portion of the spectrum of both isomers is a quartet indicating unequal coupling between H_X and the two methylene protons, labeled H_A and H_B. Since the chemical shift of H_X is too close to those of H_A and H_B to permit an ABX analysis, values for J_{AX} (8.0 and 7.5) and J_{BX} (3.2 and 3.4) were estimated by a first-order analysis of the downfield quartet side band of the H_X proton signal. Although these values are probably not as accurate as listed, in view of the difficulty of locating the necessary signals accurately, the important point is that J_{AX} and J_{BX} differ by at least a factor of 2. Chemical shifts and spin coupling constants of histidine and its *cis* and *trans* 2:1 complexes are summarized in Table VII.

Complexes of S-Alkyl-Substituted Amino Acids. The spectrum of $Pt(S\text{-}Me\text{-}L\text{-}Cys)(ND_3)_2Cl$, shown in Figure 9, is typical of the spectra obtained for all 1:1

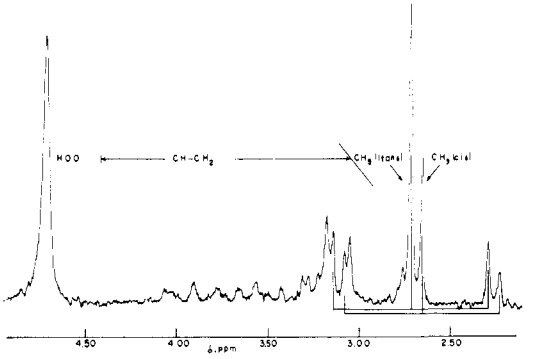

Figure 9. Proton nmr spectrum of $Pt(S\text{-}Me\text{-}L\text{-}Cys)(ND_3)_2Cl$ in D_2O showing presence of both *cis* and *trans* isomers.

complexes of S-methylcysteine. The complexity of the spectrum is greatly increased by two factors, (1) the presence of two isomers by virtue of the asymmetry resulting from coordination to S and (2) the presence of ^{195} Pt side bands for all six protons, as expected for bidentate coordination through S and N. The presence of two isomers is revealed particularly clearly by the appearance of the methyl resonance signal. It consists of two overlapping 1:4:1 triplets. The relative areas of the two triplets are about in the ratio 2:1. We have tentatively assigned the larger peaks to the

Table VIII. Proton Nmr Data for S-Methyl-L-cysteine, Methionine, and Pt(II) Complexes

Principal species	δ_{CH}	δ_{CH_2}	δ_{CH_3}	δ_{en-CH_2}	$J_{Pt-S-CH_3}$	$J_{Pt-en-CH_2}$
H_2S-MeCys$^+$	4.43	3.25	2.23			
HS-MeCys	4.07	3.14	2.23			
S-MeCys$^-$	3.52	2.85	2.18			
HPt(S-MeCys)Cl_2	?		2.74		55.2	
Pt(S-MeCys)Cl_2^-	3.96	3.22	2.75		55.6	
			2.71		55.6	
cis-HPt(S-MeCys)NH_3Cl^+ [a]	?	3.14	2.71		44.0	
			2.65		44.5	
Pt(S-MeCys)$(NH_3)_2^+$	3.86	3.14	2.74		50.8	
			2.68		50.8	
Pt(S-MeCys)en$^+$	3.85	3.12	2.73	2.82	51	42
			2.67		51	
H_2Met$^+$			2.22			
HMet			2.20			
Met$^-$			2.17			
HPtMetCl_2			2.65[b]		54	
cis-PtMetNH_3Cl^+ [a]			2.62[b]		45	
Pt$Met(NH_3)_2^+$			2.60[b]		50.5	

[a] *cis* refers to the two coordinated nitrogen atoms. [b] Although the CH_3 signal is split into a doublet, the extent of the splitting is small (<1 Hz) so that separate values are not listed.

isomer in which CH_3 and CO_2^- are *trans*, since their frequencies are less affected by protonation of the CO_2^- group. It has so far not been possible to account satisfactorily for all the lines in the CH–CH_2 portion of the spectrum. A deceptively clean doublet is usually present in the CH_2 region and a corresponding triplet is sometimes observed for the CH region. The implied equality of coupling of methine to both methylene protons is surprising, but not impossible. However, we have not succeeded in assigning the remaining peaks to ^{195}Pt side bands to complete the analysis, as we were able to do for diaminopropionic acid complexes. The problem is complicated by the fact that CH_2 peaks overlap CH_3 side bands and *vice versa*.

Chemical shifts and spin coupling constants of S-methylcysteine and its Pt(II) complexes are summarized in Table VIII. Methyl proton data are also included for some corresponding methionine complexes for comparison.

For S-ethylcysteine complexes, similar chemical shifts and overlapping and complicated side bands of two different CH_2 groups precluded complete analysis of the spectra. However, the presence of two methyl triplets, separated by about 0.05 ppm and in a 2:1 ratio, confirmed the presence of isomers in about the same ratio found for S-methylcysteine complexes.

Discussion

Mechanism of Equilibration of $PtGly_4^{2-}$ and $PtCl_4^{2-}$. In interpreting the equilibration data the reaction scheme shown in Figure 10 was considered. In this scheme, N represents N-coordinated glycinate; NO, chelated glycinate. For all 2:1 complexes, both *cis* and *trans* isomers need to be considered. It is assumed that glycinate is either N-coordinated or chelated in the mid-pH range where these experiments were run. The equilibration experiments suggest the following mechanism for the equilibration. (1) PtN_4^{2-} loses Gly$^-$ to form PtN_2NO^-. (2) The Gly$^-$ reacts rapidly with $PtCl_4^{2-}$ to yield $PtCl_2NO^-$, probably *via* $PtCl_3N^{2-}$, which never builds up to an observable level. For $PtGly_4^{2-}$–$PtCl_4^{2-}$ ratios near 1:1, steps 1 and 2 are relatively fast. (3) *cis*-$Pt(NO)_2$ is then probably produced more slowly by loss of one N-coordinated Gly$^-$ from PtN_2NO^-. (4) *trans*-$Pt(NO_2)$ is produced by the rapid addition of the released Gly$^-$ to $PtCl_2NO^-$. In summary, under the conditions of the experiments, any species containing N-coordinated glycinates and Cl^- is unstable with respect to the chelated species with one less chloride.

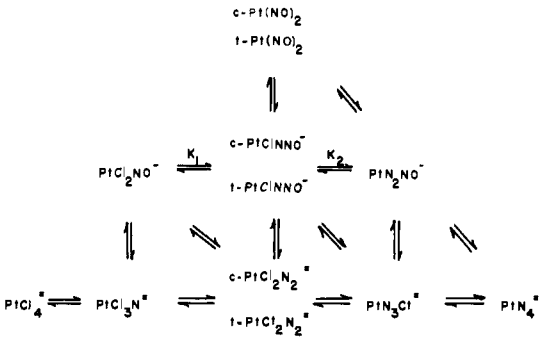

Figure 10. Equilibria and reaction pathways for the system $PtCl_4^{2-}$–$PtGly_4^{2-}$. NO and N represent chelated and N-coordinated glycinate, respectively.

Effect of Coordination on Chemical Shifts. Coordination to Pt invariably produces substantial downfield shifts for ligand protons. The extent of the downfield shift is similar to corresponding protonation shifts and decreases similarly with distance from the coordination site. Among the methyl-substituted glycines, chelation produces a downfield shift about 80% as great as that resulting from single protonation. Not surprisingly, CH_2 signals of N-coordinated glycinates are shifted downfield only half as much as those of chelated glycinates, but are much more affected by protonation of the free CO_2^- group.

Such observations are the basis for concluding that the α-carboxyl group, rather than the β-carboxyl group, is involved in chelation to Pt in complexes of L-aspartate. For those complexes, the methine proton is more affected by complexing, while the methylene protons are more affected by subsequent titration of the uncomplexed carboxyl. For S-methylcysteine, and

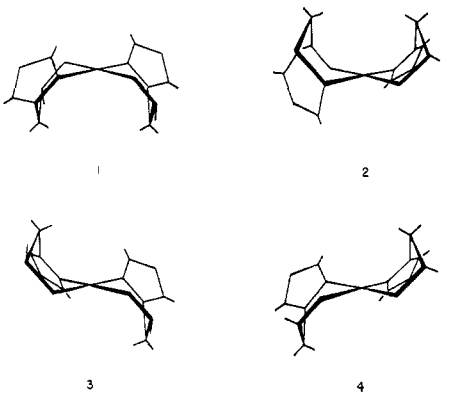

Figure 11. Conformational representations of 2:1 histidine complexes of Pt(II) showing relative orientation of the five skeletal protons: 1, *trans* isomer, α conformation; 2, *trans* isomer, β conformation; 3, *cis* isomer, α conformation; 4, *cis* isomer, β conformation.

methionine, the effect of protonation of NH_2 and CO_2^- on CH_3 shifts is not large, but coordination of NH_2 to Pt produces a downfield shift comparable to the effect of protonation or complexing N for N–CH_3 groups.

Differences in chemical shifts for all ligand protons were negligible for the following pairs of isomers: *trans*-Pt(L-Asp)$_2$ and Pt(L-Asp)(D-Asp), *trans*-Pt(L-Glu)$_2$ and Pt(L-Glu)(D-Glu), and *cis*- and *trans*-Pt(L-Dap)$_2$. For Pt(L-Hist)$_2$, chemical shifts of *cis* and *trans* isomers are very similar for corresponding protons of corresponding species, except for C_2–H whose environment in the two isomers varies significantly.

Platinum–Proton Coupling and Coordination. The presence or absence of Pt side bands provides a clear indication of the site of coordination in these complexes. In general, three-bond Pt–N–C–H couplings are between 10 and 60 Hz. Coupling through four bonds is negligibly small, except for C_4–H of histidine which is coupled through four bonds nearly as strongly as is C_2–H through three bonds.[32]

Not surprisingly, in view of the known strong tendency of Pt(II) to coordinate sulfur, $J_{Pt-S-C-H}$ values are generally among the largest values observed. A small, but noteworthy, variation in J_{Pt-CH_3} was observed for 1:1 complexes of both S-methylcysteine and methionine. Starting with Pt(AA)Cl_2, replacement of the Cl *cis* to the N of AA by NH_3 decreases J_{Pt-CH_3} from ~55 to ~45 Hz, while replacement of both Cl's by NH_3 or by ethylenediamine has a smaller effect (~55 to ~50 Hz).

Conformational Implications. For L-Dap and L-Hist complexes the nmr data provide a clear indication of the preferred conformation of the coordinated ligand.

The most likely conformation of coordinated Dap is 7, which places the bulky CO_2H group in a pseudo-equatorial position. In this conformation, one of the

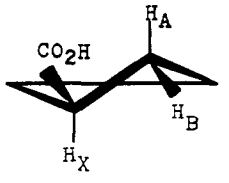

7

methylene protons is approximately *trans* to H_X while the other is approximately *gauche*. Assuming a Karplus-type dependence of J_{vic}, the axial proton, designated H_A, would be the methylene proton which is coupled more strongly to H_X (9.8, 9.2 Hz), while the equatorial proton, designated H_B, would be the one which is coupled less strongly to H_X (4.8, 4.7 Hz).

The fact that the protonated forms of both *cis* and *trans* isomers have very similar values for these parameters indicates that the conformation of one ligand is not significantly dependent on the presence or stereochemistry of the other ligand moiety in the molecule. Since both neutral and cationic forms of the more soluble isomer have almost identical spin-coupling constants, the conformation of the coordinated ligand must also be virtually unaffected by the state of ionization of the free carboxyl group; *i.e.*, the conformation must be determined primarily by steric rather than electrostatic factors.

The conformation indicated by proton–proton spin coupling constants requires that the Pt–N–C–H dihedral angles for H_A and H_X are equal (about 90°) while the corresponding angle for H_B is about 150°. Similarly, $J_{Pt-H_A} = J_{Pt-H_X}$ (30 ± 1 *vs.* 28 ± 2 Hz) while $J_{Pt-H_B} = 55 \pm 1$ Hz. Although it is certainly an oversimplification to attribute these differences to a simple Karplus-like dependence for J_{Pt-H} in Pt–N–C–H fragments, for these angles, corresponding proton–proton coupling constants would also differ considerably, with $J_{150} > J_{90}$.

Turning to histidine complexes, two possible conformations need to be considered. Because of the conformational restrictions of the imidazole ring, histidine ligands coordinated through amine and imidazole nitrogens must be in one of two boat conformations. Assuming that one or the other conformation prevails for both ligand fragments, the two conformations of each isomer of Pt(L-Hist)$_2$ are shown in Figure 11. Only the five protons which are observed in the nmr spectra are explicitly indicated. The conformation in which the carboxyl group lies below the floor of the boat is designated the α conformation and above the floor, the β conformation.

The nmr data indicate that the α conformation predominates for the fully protonated cation, while the β conformation predominates for the negatively charged anion at high pH. The conclusion that the histidine ligand is in the α conformation at low pH is based on the equality of coupling between H_X and H_A, H_B (~4.6 Hz). In the α conformation the dihedral angles between H_X and the two methylene protons are both 60°, which would lead to equal and relatively small coupling. By contrast, at high pH, where protons have been removed from both carboxyl groups and imidazole rings, H_X is coupled much more strongly to one of the two methylene protons (~8 *vs.* ~3 Hz), as would be expected for the β conformation, in which one of the methylene protons is *trans* to H_X. These conclusions hold for both *cis* (less soluble) and *trans* (more soluble) isomers. Unfortunately, the low solubility of the neutral species of both isomers made it impossible to draw any conclusions about the conformation of that form.

It is of interest to compare the conformational situations of Pt(L-Dap)$_2$ and Pt(L-Hist)$_2$. For the former,

(32) *Cf.* P. D. Kaplan and M. Orchin, *Inorg. Chem.*, **4**, 1393 (1965); P. S. Braterman, *ibid.*, **5**, 1085 (1966), and ref 19 and 20.

the same conformation, dependent on the bulkiness of the CO_2H (or CO_2^-) group, appears to prevail for both cationic and neutral forms. For the latter, the α conformation which allows maximum removal of CO_2H from the Pt atom is more important for the cationic form, but the β conformation prevails for the anionic species. In the β conformation, the two negative charge centers in each ligand moiety, CO_2^- and imidazole ring, are separated to a maximum extent. Thus for both compounds, the conformation in which the carboxyl group is far away from the Pt atom prevails unless electrostatic repulsion between negatively charged groups in *the same* ligand moiety becomes important. The presence or conformation of a second ligand seems to have little influence on the conformation of the other ligand. The latter conclusion is supported also by the chemical shift data. Except for C_2–H of histidine, whose environment is much different in the *cis*- and *trans*-Pt(L-Hist)$_2$ isomers, all protons have essentially identical chemical shifts for corresponding species.

The dihedral angle dependence of J_{Pt-H} indicated by the foregoing analysis provides a basis for determining the preferred conformation for some of the other ligands whose spectra have been described. The complexes of sarcosine, aspartic and glutamic acids, and EDTA will be considered in more detail.

For the sarcosine complex $PtSarCl_2^-$, the difference between the two methylene protons is much less than the difference between methylene protons of Dap complexes. The proton which is more shielded (upfield) is also the proton which is coupled more strongly to ^{195}Pt and less strongly to the N–H proton. Since the coupling constant differences are small, it is likely that there is no strong preference for any one conformation. Nevertheless, there is a substantial difference in the chemical shifts of the two methylene protons. Any suggestion as to a preferred conformation must be consistent with all three observations. On that basis, we feel that conformation **8** is more significant than the alternative which has the CH_3 group in a pseudo-equatorial conformation. The proton designated H_A

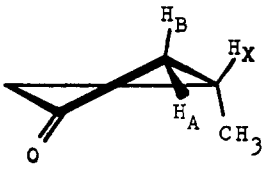

8

is more nearly *trans* to the Pt and should be more weakly coupled to H_X. Furthermore, the magnetic anisotropy of both the C–N and C=O bonds should increase the shielding of H_A while decreasing the shielding of H_B.[33]

For aspartic and glutamic acids, the choice of a preferred conformation is based entirely on the magnitude of the coupling between ^{195}Pt and the α proton. For

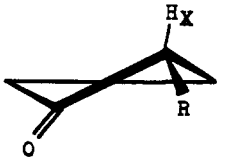

9

(33) J. I. Legg and D. W. Cooke, *Inorg. Chem.*, 4, 1576 (1965).

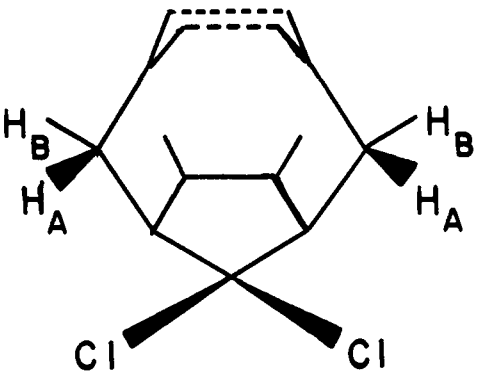

Figure 12. Proposed preferred conformation of $H_4Pt(EDTA)Cl_2$ in D_2O based on proton nmr spectrum.

the aspartic acid complexes, this value is relatively small (20 cps), suggesting that conformation **9** predominates. For glutamic acid complexes, the values are somewhat larger, but are still comparable to the smaller values observed for Dap complexes. Perhaps the negatively charged carboxyl group is more strongly repelled the shorter the hydrocarbon chain. In any case, it is clear that chelated aspartic and glutamic acids both exist predominantly in the conformation which places the bulky $(CH_2)_n$–CO_2^- group in an equatorial position.

In contrast to all of the cases considered up to this point, in which the conformation of a chelate ring was considered, for the bidentate complex $H_4Pt(EDTA)Cl_2$ the nmr data indicate the preferred conformation of the free acetate fragments. The preferred conformation suggested by the data is shown in Figure 12. Only one-half of the structure is shown, so as to emphasize the important features. The proposed conformation could be stabilized by internal hydrogen bonds (dotted lines) between carboxyl groups of acetate fragments attached to *separate* nitrogens. In the proposed conformation, one of the two methylene protons is *trans* to Pt while the other is *gauche*, accounting for the large differences in J_{Pt-H} (46 *vs.* 11 Hz).

Finally, there are the $H_2Pt(EDTA)$ data, which can best be accounted for in terms of substantial puckering of the chelated acetate ring resulting in the large difference between J_{Pt-H_A} and J_{Pt-H_B} (58 *vs.* 6 Hz), where H_A is the equatorial proton (*trans* to Pt) while H_B is the axial proton (*gauche* to Pt).

The dihedral angle (ϕ) dependence of J_{Pt-H} indicated by these data is summarized in Table IX. Data are

Table IX. The Dihedral Angle Dependence of J_{Pt-H} in Pt–N–C–H Fragments

Species	Proton	Estimated ϕ	Obsd J, Hz
$H_4Pt(EDTA)Cl_2$	H_B (ac)	180	46
$H_2Pt(EDTA)$	H_A (chel-ac)	180	58
$H_2Pt(L\text{-}Dap)_2^{2+}$	H_A	150	55
$Pt(L\text{-}Hist)_2^{2-}$	H_X	140	44
$H_2Pt(L\text{-}Hist)_2^{2+}$	H_X	120	33
$H_2Pt(L\text{-}Dap)_2^{2+}$	H_X, H_B	90	30
$H_4Pt(EDTA)Cl_2$	H_A (ac)	60	11
$H_2Pt(EDTA)$	H_B (chel-ac)	60	6

included only for the complexes for which one extreme conformation appears to prevail. The data suggest that J approaches a maximum for $\phi = 180°$ and a

minimum for $\phi = 0°$. The pattern is similar to that noted by Keevoy[34] for vicinal $^{1}H-^{199}Hg$ couplings in a variety of Hg compounds.

Suggestions for Further Work. The conformation dependence of J_{Pt-H} in Pt–N–C–H fragments indicated by these data suggests further experiments, in addition to application to other ligands. A more thorough investigation of platinum complexes of other ligands of known geometry could be carried out to establish the dependence more precisely. In particular, the details of the dependence as ϕ approaches zero should be further investigated. Such investigations could also include complexes of other spin one-half nuclei (*e.g.*, ^{57}Fe, ^{89}Y, ^{103}Rh, ^{107}Ag, ^{109}Ag, ^{111}Cd, ^{113}Cd, ^{169}Tm, ^{171}Yb, ^{183}W, ^{203}Tl, ^{205}Tl, ^{207}Pb) to determine the generality of the phenomenon.

(34) M. M. Keevoy and J. F. Schaefer, *J. Organometal. Chem.*, **6**, 589 (1966).

Acknowledgments. The authors wish to thank Dr. Richard Ernst and the University of Wisconsin for obtaining 100-MHz spectra and Mr. Stephen Schneider for preparing samples of the EDTA complexes. This investigation was supported by Public Health Service Research Grant No. CA-06852 from the National Cancer Institute and by the National Science Foundation, Grant No. GY-8064 and GY7.

The Secondary *trans* Effect in Platinum(II) Complexes[1]

George W. Watt and Willis A. Cude

Contribution from the Department of Chemistry, The University of Texas at Austin, Austin, Texas 78712. *Received May 10, 1968.*

Abstract: Existence of a secondary *trans* effect in platinum(II) complexes has been established unequivocally by deprotonation and subsequent methylation of ions of the type $[Pt(dien)X]^+$ where $X^- = I^-$, CSN^-, and NO_2^-. The methylation of [Pt(dien-H)X] proceeds at differing rates which permits the ordering of the base strength of the deprotonated species as $I^- > SCN^- > NO_2^-$ for these ligands as X^-.

Palmer and Basolo[2] have reported results which suggested that the *trans* effect is observable not only in metal–ligand bonds but also in the bonding of atoms attached to a coordinated ligand atom. They measured two separate rates for the amine hydrogen exchange for ions of the general formula $[Pt(dien)X]^+$, where X = ligands with a single negative charge, and associated the faster rate with the hydrogen of the secondary amino group *trans* to the ligand X. It therefore became of interest to determine if this observed difference in exchange rates represented enough difference in actual chemical reactivity so that a selective deprotonation could be accomplished at a site on the coordinated diethylenetriamine that is normally less reactive than the four other possible reaction sites. To this end, ions of the same type as used by Palmer and Basolo were synthesized and treated with NH_2^- in liquid ammonia solution in an attempt to determine if such selective deprotonation could indeed be demonstrated. Such deprotonation would provide direct chemical evidence that a secondary *trans* effect does extend beyond the metal–ligand atom bond to atoms attached to the coordinated ligand atom.

Results and Discussion

Before attempting any deprotonation reactions, it was necessary to test the stability of $[Pt(dien)X]^+$ in liquid ammonia solution. As indicated in the Experimental Section, the ions were more soluble in NH_3 than in H_2O, and ammoniation occurred to produce $[Pt(dien)NH_3]^{2+}$ for $X^- = Cl^-$ and Br^-, while for $X^- = I^-$, NO_2^-, and SCN^- the complex could be recovered from solution unchanged. Inasmuch as the latter three ligands have approximately the same order and are two orders of magnitude greater than NH_3 for their *trans* effect,[3] only those ions containing I^-, NO_2^-, and SCN^- were suitable for deprotonation studies.

It was predicted[4] that the deprotonation site of [Pt(dien-H)X] could be established upon isolation of these compounds using infrared spectra as a diagnostic tool. Such, however, was not found to be the case as is evident from the spectra illustrated in Figure 1 along with the tentative assignments made in Table I. The latter were made empirically on the basis of the assignments previously made[4] for [Pd(dien)I] I since there was almost a 1:1 correlation between the spectra of the Pt and Pd complexes. Comparison of the spectra in Figures 1a and b suggests that the deprotonation occurred on the center nitrogen of dien since the two surviving peaks at 3180 and 3120 cm^{-1} correspond almost exactly to the $\nu(NH_2)$ peaks at 3200 and 3130 cm^{-1} in the starting compound. The broad, ill-defined nature of the NH_2 stretching bands in the deprotonated species precludes any unequivocal statement that the ν(NH) peak at 3070 cm^{-1} in the starting compound has disappeared. The out-of-plane deformation for the NH group at 1440 cm^{-1} in [Pt(dien)I] I might also have been obscured in the spectra of the deprotonated species, in this case by the general

(1) Abbreviations used in this paper: dien, diethylenetriamine, where the nitrogens are designated N^1, N^2, and N^3; 2-mdien, N^2-methyldiethylenetriamine; 1-mdien, N^1-methyldiethylenetriamine; dien-H, diethylenetriamine from which a proton has been removed; n-mdien, methyldiethylenetriamine in which no specification is made as to the nitrogen to which the methyl group is bonded.

(2) J. S. Palmer and F. Basolo, *J. Phys. Chem.*, **64**, 778 (1960).

(3) F. Basolo and R. G. Pearson, "Mechanisms of Inorganic Reactions," 2nd ed, John Wiley and Sons, Inc., New York, N. Y., 1967.

(4) G. W. Watt and D. S. Klett, *Spectrochim. Acta*, 20, 1053 (1964).